

Article

Synthesis and Self-assembly of Discrete Dimethylsiloxane-Lactic Acid Diblock Co-oligomers; the Dononacontamer and its Shorter Homologues

Bas Van Genabeek, Bas F.M. de Waal, Mark M.J. Gosens,
Louis M. Pitet, Anja R.A. Palmans, and E. W. Meijer

J. Am. Chem. Soc., **Just Accepted Manuscript** • DOI: 10.1021/jacs.6b00629 • Publication Date (Web): 08 Mar 2016

Downloaded from <http://pubs.acs.org> on March 9, 2016

Just Accepted

"Just Accepted" manuscripts have been peer-reviewed and accepted for publication. They are posted online prior to technical editing, formatting for publication and author proofing. The American Chemical Society provides "Just Accepted" as a free service to the research community to expedite the dissemination of scientific material as soon as possible after acceptance. "Just Accepted" manuscripts appear in full in PDF format accompanied by an HTML abstract. "Just Accepted" manuscripts have been fully peer reviewed, but should not be considered the official version of record. They are accessible to all readers and citable by the Digital Object Identifier (DOI®). "Just Accepted" is an optional service offered to authors. Therefore, the "Just Accepted" Web site may not include all articles that will be published in the journal. After a manuscript is technically edited and formatted, it will be removed from the "Just Accepted" Web site and published as an ASAP article. Note that technical editing may introduce minor changes to the manuscript text and/or graphics which could affect content, and all legal disclaimers and ethical guidelines that apply to the journal pertain. ACS cannot be held responsible for errors or consequences arising from the use of information contained in these "Just Accepted" manuscripts.



ACS Publications

Synthesis and Self-assembly of Discrete Dimethylsiloxane-Lactic Acid Diblock Co-oligomers; the Dononacontamer and its Shorter Homologues

Bas van Genabeek, Bas F. M. de Waal, Mark M. J. Gosens, Louis M. Pitet, Anja R. A. Palmans, and E. W. Meijer*

Institute for Complex Molecular Systems and Laboratory of Macromolecular and Organic Chemistry, Eindhoven University of Technology, P.O. Box 513, 5600 MB Eindhoven, the Netherlands

Block copolymer, self-assembly, monodisperse, oligomer, polydimethylsiloxane, polylactic acid, molar mass distribution, precision synthesis.

ABSTRACT: Most of the theoretical and computational descriptions of the phase behaviour of block copolymers describe the chain ensembles of perfect and uniform polymers. In contrast, experimental studies on block copolymers always employ materials with disperse molecular makeup. Although most polymers are so-called monodisperse, they still have a molecular weight dispersity. Here, we describe the synthesis and properties of a series of discrete length diblock co-oligomers, based on oligo-dimethylsiloxane (*o*DMS) and oligo-lactic acid (*o*LA); diblock co-oligomers with highly non-compatible blocks. By utilizing an iterative synthetic protocol, co-oligomers with molar masses up to 6901 Da, ultra-low molar mass dispersities ($\bar{D} \leq 1.00002$), and unique control over the co-oligomer composition are synthesized and characterized. This specific block co-oligomer required the development of a new divergent strategy for the *o*DMS structures by which both bis- and monosubstituted *o*DMS derivatives up to 59 Si-atoms became available. The incompatibility of the two blocks makes the final coupling more demanding the longer the blocks become. These optimized synthetic procedures granted access to multi-gram quantities of most of the block co-oligomers, useful to study the lower limits of block copolymer phase segregation in detail. Cylindrical, gyroid, and lamellar nanostructures, as revealed by DSC, SAXS and AFM, were generated. The small oligomeric size of the block co-oligomers resulted in exceptionally small feature sizes (down to 3.4 nm) and long-range organization.

■ INTRODUCTION

Block copolymers (BCPs) are an intensively studied class of materials exhibiting a broad application window. The propensity to self-organize into various morphological structures having segregated domains on the length scale of individual-chain dimensions makes such materials ideally suited for various nanotechnologies. Lithographic resists for nanoscale patterns,^{1–9} ultrafiltration membranes,^{10–12} stimuli-responsive materials,¹³ and next-generation organic solar cells¹⁴ highlight only few of these possible applications. Of the many different BCPs synthesized and studied, diblock copolymers are the ones that attracted most attention.

Diblock copolymers comprise two chemically distinct polymeric segments, consisting generically of A and B monomers, respectively, and linked together by a single covalent connection. Three important physical parameters dictate the self-organizing behaviour of diblock copolymers: the Flory-Huggins interaction parameter, χ ; the overall degree of polymerization, N ; and the polymer composition, expressed as the volume fraction of block A (f_A) or block B (f_B).¹⁵ The thermodynamic immiscibility of the blocks, reflected by χ , has typical values between 0.02 and 0.4. The interaction parameter is an intrinsic property of a given block combination. On the

contrary, N , f_A and f_B are variables established via synthetic control.

Several theoretical studies have emerged that enable simulations to predict accurately the properties and self-assembly behaviour of diblock copolymers.^{16–20} However, relatively few models have accounted for chain-length dispersity, as result of the disproportionately longer calculation times typically required for disperse systems.^{21–24} On the contrary, almost every reported synthetic diblock copolymer, although called monodisperse, exhibits molar mass dispersity to a certain extent due to remaining challenges in preparing well-defined polymers.²⁵ This dispersity is a direct and inevitable result of the living polymerization procedures typically employed to produce diblock copolymers. Next to dispersities in molar mass (hence in N), dispersities in the composition (hence in f_A versus f_B) further disconnect theory and experiments. In some cases, separation techniques, like recycling GPC, were successful to minimize these dispersities in diblock copolymers.²⁶ Remarkably, to our knowledge, there is only a limited number of examples of uniform synthetic block copolymers with high χ -parameter reported to date.^{27,28} Perfectly uniform polymers are ideal candidates to study the chain length dependence of the polymer properties and to substantiate results from simulations and the underlying theoretical concepts.

Still, even the list of reported uniform, linear homopolymers and oligomers with more than 20 repeating units—excluding the biological structures made by solid-phase synthesis—is remarkably short; covering (un)branched olefins,^{29–32} oligoethylene glycols,^{33–39} polyethers,^{40,41} polyesters^{42–45} and conjugated oligomeric systems.^{46–50} Every oligomer/polymer required its own synthetic approach, typically divided into either a divergent or a convergent approach, similar to the synthesis of dendrimers.⁵¹

Scheme 1. Conventional synthesis of disperse PDMS-*b*-PLA

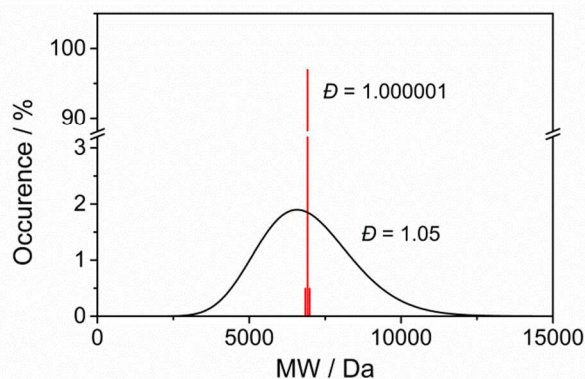
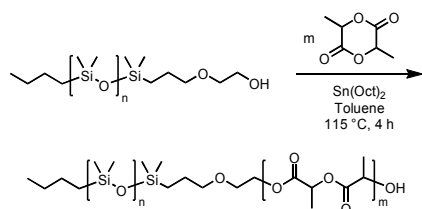


Figure 1: Graphical representation (calculated curve) of the molar mass distribution of a BCP ($M_n \approx 6.9$ kDa) with a dispersity of 1.05 (in black) and 1.000001 (in red). The y -axis region between 3 and 90% is omitted for clarity.

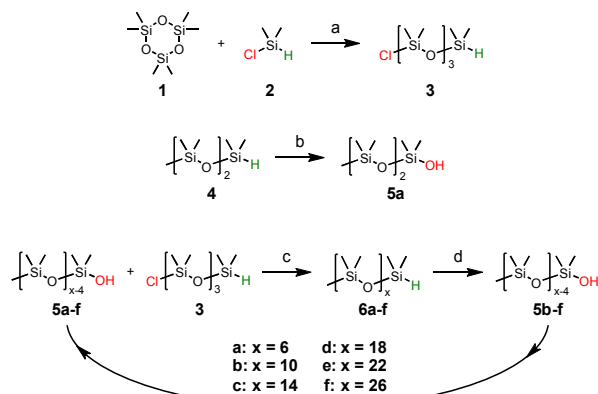
Here, we describe the synthesis and structural analysis of a series of discrete diblock co-oligomer (BCO) based on oligodimethylsiloxane (σ DMS) and atactic oligolactic acid (σ LA). Previous reports showed that these two constituents show an exceptionally high χ -parameter,³ which allows the formation of microphase-separated structures even at low N .^{6,52} The synthesis of polydimethylsiloxane-*b*-polylactide (PDMS-*b*-PLA) BCPs is conducted by stannous octoate catalysed ring-opening polymerization (ROP) of DL-lactide (LA) with a hydroxyl-terminated, low-dispersity PDMS macro-initiator (see Scheme 1). Despite being robust and fast, such polymerization techniques result in BCPs with molar mass dispersities of at least $D = 1.05$. In Figure 1, a calculated curve (Schulz–Zimm distribution) representing the molar mass distribution for a polymer a dispersity $D = 1.05$ is shown (black curve). As can be seen, this dispersity still equals a relatively broad distribution of chain lengths. Thus, a synthetic route that permits the synthesis of polymeric material with dispersities approaching unity is desirable. Since the σ DMS and σ LA blocks have such disparate chemical compatibilities and functionalities, we chose to synthesize the two discrete blocks separately.

The synthesis of homochiral, discrete length oligomers of (*S*)-lactic acid and ϵ -caprolactone has been described by Hawker and coworkers,^{44,45} which we further optimized for the fabrication of monodisperse σ LA able to couple to the σ DMS block. In addition, we developed a novel synthetic protocol to produce the discrete σ DMS blocks, since linear, discrete mass oligomers with more than eight repeating units have not been reported. Literature examples that describe the synthesis, modification or purification of oligomers based on the dimethylsiloxane building block are scarce.^{53–55} Finally, two different coupling strategies were optimized to combine the discrete homo-oligomers to furnish a library of uniform block co-oligomers, with the longest one having a total of 92 siloxane and lactic acid repeating units: *i.e.*, a dononacontamer.

RESULTS AND DISCUSSION

Synthesis of discrete length oligodimethylsiloxane blocks. The first route we developed to generate selectively discrete length oligodimethylsiloxanes (Scheme 2) focused on the formation of a bifunctional chlorosilane building block **Cl-Si₄-H (3)** with a length of four siloxane units. For convenience, we will use the following abbreviations for the σ DMS blocks: **A-Si_x-B**, where **A** and **B** represent the oligomer end groups and **Si_x** represents the number of siloxane repeating units. Using building block **3**, monodisperse σ DMS blocks were obtained by means of an iterative, two-step procedure. First, the reaction of the chlorosilane with a monofunctional, methyl end-capped silanol (**Me-Si_{x-4}-OH 5a-f**) resulted in the formation of a monofunctional silyl hydride (**Me-Si_x-H 6a-f**). After purification, this silyl hydride was converted selectively to the corresponding silanol by stirring in a phosphate buffer/dioxane mixture in the presence of a Pd/C catalyst, resulting in an increased chain length with four additional siloxane repeating units realized in two steps.

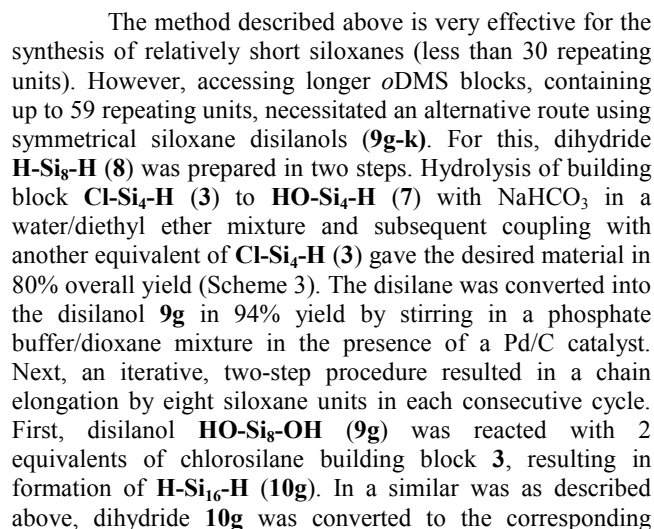
Scheme 2. Linear route for siloxane monohydrides 6a-f^a



^a Reagents and conditions: (a) ACN, DMF (cat.), RT, 70 h (55%); (b) Pd/C, dioxane, 1 M phosphate buffer (pH = 7), RT, 20 h (91%); (c) pyridine, toluene, RT, 3 h (66–99%); (d) Pd/C, dioxane, 1 M phosphate buffer (pH = 7), RT, 20 h (89–94%).

The chlorosilane building block **Cl-Si₄-H (3)** was obtained in large quantities (>100 g per batch) by ring opening of commercially available cyclotrisiloxane **1** with chlorodimethylsilane **2**. Separation of the desired material from higher mass byproducts using vacuum distillation

Scheme 3. Synthesis of longer siloxane monohydride 6l^a

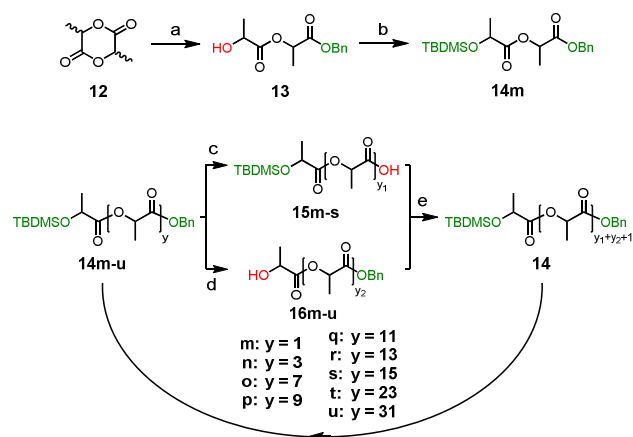


Synthesis of discrete length oligolactic acid blocks.

ACS Paragon Plus Environment

confirmed by $^1\text{H-NMR}$, $^{13}\text{C-NMR}$ and MALDI-TOF analysis. In all cases, only minor quantities (<0.5 mol%) of chains containing ± 1 repeating unit were observed.

Scheme 4. The synthesis of lactic acid oligomers 16m-u^a



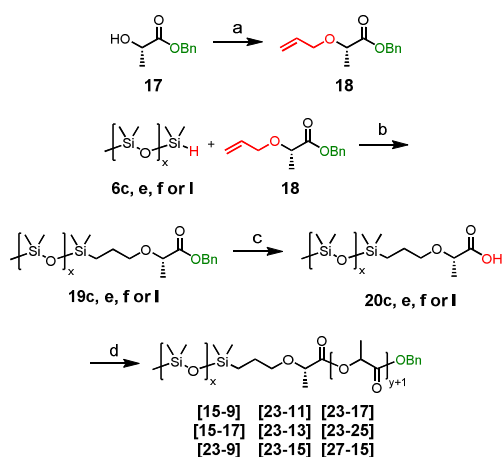
^a Reagents and conditions: (a) BnOH, CSA, toluene, 80 °C, 8 h (72%); (b) TBDMSCl, imidazole, DMF, RT, O/N (90%); (c) H_2 , Pd/C, EtOAc, RT, 2 h (quant.); (d) $\text{BF}_3 \cdot \text{Et}_2\text{O}$, DCM, RT, 4 h (88-96%); (e) EDC·HCl, DPTS, DCM, RT, 3 h (81-94%).

Synthesis of monodisperse BCOs. The coupling of the well-defined *o*DMS and *o*LA blocks to yield the final monodisperse block co-oligomers required functionalization of the *o*DMS block with a carboxylic acid end group. As shown in Scheme 5, the allyl ether of benzyl (*S*)-lactate (**18**) was obtained in moderate yield (60%) by a silver(I) oxide mediated etherification of benzyl (*S*)-lactate (**17**). Subsequently, the lactate was coupled to the *o*DMS block using the Karstedt hydrosilylation catalyst.⁵⁷ Removal of the benzyl ester by Pd/C catalysed hydrogenolysis, followed by purification with column chromatography, afforded pure and monodisperse acid functionalized *o*DMS **Me-Si_x-LA₁-COOH** (**20c, e, f and l**) having either 15, 23, 27 or 59 siloxane repeating units, respectively. Subsequent carbodiimide-facilitated ligation of this block with hydroxy-terminated *o*LA **16** of various lengths, resulted in the formation of a series of block co-oligomers [**Si-LA**] (e.g., [**23-25**] for the BCO containing 23 siloxane and 25 lactic acid repeating units; Table 1, entries 2-10). The combination of *o*DMS and *o*LA lengths were chosen such that BCOs with values for f_{LA} between 0.25 and 0.50 were obtained, with which various microstructures could be accessed. All block co-oligomers were isolated in moderate to excellent yields and in very high purity, confirmed by $^1\text{H-NMR}$, $^{13}\text{C-NMR}$ and MALDI-TOF analysis (see Figures S1-S15).

The reaction of the longest siloxane block (**Me-Si₅₉-LA₁-COOH** **20l**) with the longest *o*LA block (**HO-LA₃₂-Bn** **16u**) under similar carbodiimide coupling conditions did not give significant amounts of BCO. Instead, most of the unreacted lactic acid block was recovered. In addition, a siloxane derivative was isolated which most probably is the *N*-acylurea EDC adduct, a rearrangement byproduct that is formed as result of the slow reaction of the reactive *O*-acylurea EDC adduct with the *o*LA block. Therefore, an alternative strategy was employed to obtain

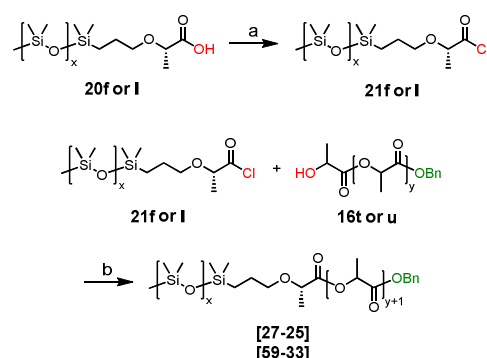
BCOs [**27-25**] and [**59-33**] (Scheme 6). Acid functionalized *o*DMS **20f or l** was transformed into the corresponding acid chloride with Ghosez's reagent.⁵⁸ Reaction of the crude acid chloride with hydroxy-terminated *o*LA **16t or u** gave the desired BCOs (Table 1, entries 11-12), albeit in low to moderate yields of 48 and 18%, respectively, after purification.

Scheme 5. Synthesis of *o*DMS-*o*LA block co-oligomers^a



^a Reagents and conditions: (a) allyl bromide, silver(I) oxide, Et_2O , reflux, O/N (60%); (b) Karstedt catalyst, toluene, 60 °C, 3h (43-75%); (c) Pd/C, EtOAc, RT, 2 h (42-81%); (d) **15**, EDC·HCl, DPTS, DCM, RT, O/N (72-96%).

Scheme 6. Alternative coupling of the blocks^a



^a Reagents and conditions: (a) Ghosez's reagent (1-chloro-*N,N*,2-trimethyl-1-propenylamine), DCM, RT, O/N (no purification); (b) dry pyridine, DCM, RT, 5 h (18-48% (two steps)).

Molecular characterization of monodisperse BCOs. Conventional size exclusion chromatography (SEC) is insufficiently sensitive for determining accurate values of co-oligomer molar mass dispersity, since all BCOs had dispersities that are far below the lower detection limit of this technique ($D \approx 1.01$). However, a striking difference was observed between the discrete length BCO [**15-17**] and a reference PDMS-PLA BCP [**Ref**] ($D = 1.15$) that was synthesized in our group before⁶ (Figure 2 and Figures S16-S18). Results that are more accurate were obtained by MALDI-TOF analysis of the BCOs, showing that co-oligomers with the expected mass were present in each sample (see Figure 3 and Figures S13-S15). Only co-oligomers [**23-17**], [**23-25**] and [**59-33**] contained traces of material that

differed from the correct co-oligomer length by one repeating unit. For those BCOs, the molar mass dispersity was estimated from the MALDI-TOF data by assuming that the relative peak intensities corresponding to the desired and undesired oligomer lengths directly represent the molar ratios of these BCOs (see Table 1; entries 8,9 and 12). For the other co-oligomers, only an upper limit of for the dispersities could be estimated, resulting in values (much) lower than 1.00001; isotope distributions not taken into account.

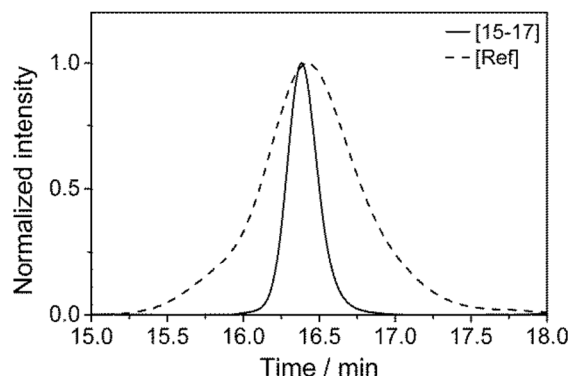


Figure 2: Normalized SEC traces (RI detector) for compounds [15-17] and [Ref].

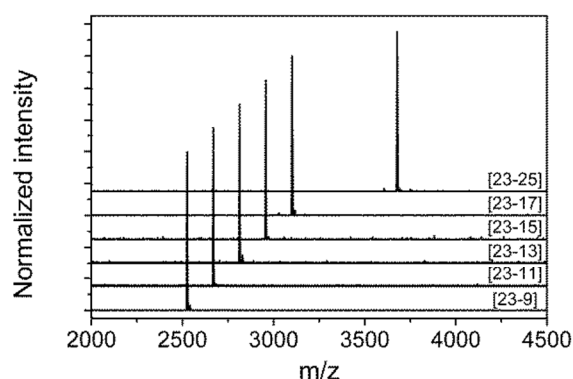


Figure 3: MALDI-TOF spectra (DCTB matrix) for the BCO series containing 23 siloxane units.

The monodisperse BCOs are chemically stable, even after long storage in ambient conditions. MALDI-TOF analysis of samples that were stored in air for 6 months at room temperature did not show any degradation product. Furthermore, the thermal stability of the BCOs was further investigated with thermogravimetric analysis (TGA). The start of the degradation onset at temperatures close to 300 °C highlighted the remarkable stability for a polyester containing material (Figure S19).

Differential scanning calorimetry (DSC) was used to investigate the dependence of chain length on the thermal transitions of the new block co-oligomers (see Figure 4 and Figures S20-S21). Although the glass transition temperature of the *o*DMS block was too low (< -50 °C) to be observed with our available DSC set-up, the glass transition of the *o*LA block was evident, with values for T_g (*o*LA) between -32.7 °C and +9.1 °C, monotonically increasing with increasing f_{LA} (Table

1). Furthermore, the T_g values found for *o*LA blocks in the BCOs are much lower than those found for the pure *o*LA blocks (e.g., for **HO-LA₁₆-Bn** (**16s**) a T_g of 19.1 °C was found). In addition, all block co-oligomers, except the shortest, [15-9], showed a second thermal transition at higher temperatures (indicated with an asterisk in Figure 4). This endothermic transition is attributed the order-disorder transition (ODT) in which the phase segregated state goes into the isotropic melt, a transition that is rarely observed in DSC analyses of block copolymers.^{7,8,59,60} Small-angle X-ray scattering (SAXS) experiments (*vide infra*) confirm that the samples are phase segregated and well-organized at temperatures below the T_{ODT} . As expected, T_{ODT} increases in the DSC experiments with increasing chain length for the BCOs with similar f_{LA} : [15-17], [23-25] and [27-25] (Table 1; entries 3, 9 and 11, respectively). Interestingly, when using a heating and cooling rate of 10 °C min⁻¹, sharp ODT signatures were obtained for co-oligomers [15-17] and [23-25] (less than 1 °C broad). However, in the BCOs with a lower f_{LA} , this transition was broadened over a 5–6 °C temperature range. The use of a temperature ramp of 5 °C min⁻¹ did not change the results significantly. Currently, the origin of this behaviour is under investigation.

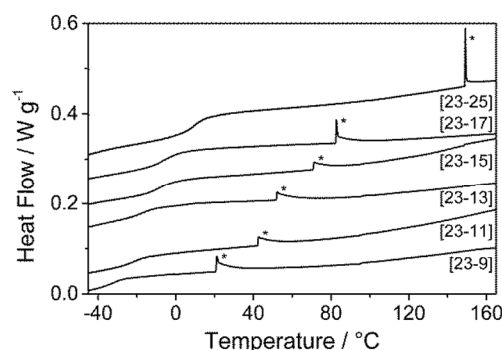


Figure 4: DSC traces (second heating run) of the BCOs containing 23 siloxane units. The data is shifted for clarity. Order-disorder transitions are indicated with an asterisk (*). A heating/cooling rate of 10 °C min⁻¹ was used.

Determination of BCO microstructures. After confirming the purity and thermal properties of the uniform block co-oligomers synthesized, the micro-phase separation was analysed in bulk with small-angle X-ray scattering and as a thin film with atomic force microscopy.

Bulk morphologies. Small-angle X-ray scattering at room temperature was used to determine the bulk morphology and principal domain spacing (d^*) for all BCO samples (Table 1). Azimuthal integration of the 2-D transmission scattering data resulted in 1-D patterns. A selection of data collected at 20 °C is shown in Figure 5, representing 3 of the 4 classical BCP morphologies and a disordered state. The scattering profile of the short, compositionally asymmetric BCOs with a low f_{LA} value, [15-9] and [23-9] (Figure S22), showed only low intensity and broad principal scattering peaks at 1.17 and 1.03 nm⁻¹, respectively. This suggests that these co-oligomers are disordered, with only a weak composition inhomogeneity present at room temperature. Furthermore, repeating the measurement at -5 °C did not result in any additional ordering for either sample. This is in accordance with the absence of an ODT in the DSC trace of compound [15-9]. However, the

presence of an ODT signature for the [23-9] BCO at 20.7 °C suggests that this co-oligomer should adopt a more ordered state at -5 °C. At this moment we have no viable explanation

for this observation, although we presume that it is related to kinetic effects.⁶⁰

Table 1: Molecular characterization data for monodisperse block co-oligomers.

Entry	Co-oligomer ^[a]	M_n [Da]	$N^{[b]}$	$f_{LA}^{[c]}$	$\bar{D}^{[d]}$	$T_g^{[e]}$ [°C]	$T_{ODT}^{[f]}$ [°C]	Phase ^[g]	d^* ^[h] [nm]
1	[Ref]	2554 ^[i]	33.5	0.46	1.15 ^[j]	n.d.	n.d.	DIS	-
2	[15-9]	1909	25.6	0.34	< 1.00001	-32.7	-	DIS	-
3	[15-17]	2486	32.6	0.48	< 1.00001	0.5	72.9	LAM ^[k]	6.8
4	[23-9]	2502	35.0	0.25	< 1.00001	-32.0	20.7	DIS	-
5	[23-11]	2646	36.8	0.29	< 1.00001	-21.1	42.2	CYL ^[k]	6.5
6	[23-13]	2791	38.5	0.32	< 1.00001	-17.2	52.3	CYL	7.1
7	[23-15]	2935	40.3	0.35	< 1.00001	-7.6	70.8	GYR	7.4
8	[23-17]	3079	42.0	0.37	1.00001	-6.8	82.5	GYR	7.8
9	[23-25]	3655	49.0	0.46	1.00001	9.1	148.9	LAM	8.7
10	[27-15]	3231	45.0	0.31	< 1.00001	-6.6	91.3	CYL	8.0
11	[27-25]	3952	53.7	0.42	< 1.00001	5.8	151.3	LAM	9.3
12	[59-33]	6901	98.5	0.30	1.00002	n.d.	n.d.	CYL	13.7

[a] Number of repeating siloxane and lactic acid units respectively; [b] Number of segments based on an 118 Å³ reference volume; [c] Lactic acid volume fraction, calculated using bulk densities for PDMS and PLA (0.95 g/ml and 1.24 g/ml, respectively); [d] Calculated from the relative peak intensities in the MALDI-TOF spectra; [e] Glass transition of the *o*LA block; [f] Order-disorder temperature; [g] Bulk morphology determined with SAXS at room temperature. DIS = disordered, CYL = cylindrical, GYR = gyroid, LAM = lamellar; [h] Domain spacing, calculated as $d^* = 2\pi/q^*$; [i] Calculated from ¹H-NMR integral ratios; [j] Determined by SEC; [k] After aging for 6 months at room temperature; n.d. = not determined

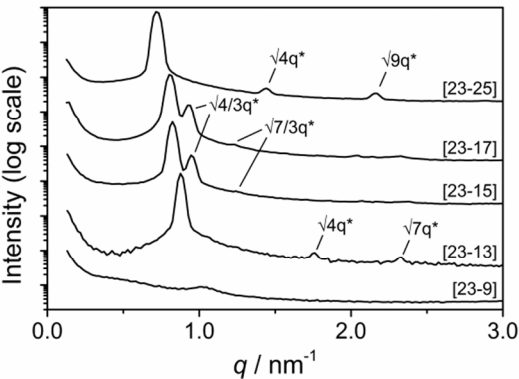


Figure 5: SAXS data for the BCOs containing 23 siloxane units. The data is shifted vertically for clarity. Higher order Bragg reflections are indicated if present.

It is important to note here that the scattering profile of the disperse polymer [Ref] ($\bar{D} = 1.15$) lacks any evidence for phase segregation or composition fluctuations, even though this polymer has a comparable χN value. In contrast, the scattering profile of the BCO [15-17] with similar lengths of both blocks was dominated by a very narrow, high intensity principal peak at $q^* = 0.93 \text{ nm}^{-1}$ (Figure S23). Still, the absence of higher order reflections suggested that the presence of this scattering peak merely is a result of very strong composition fluctuations in the bulk material, lacking any long-range ordering. Interestingly, repetition of the scattering experiment with a sample that was stored in a glass capillary at room temperature for 6 months⁶¹ revealed additional reflections at $\sqrt{4}q^*$ and $\sqrt{9}q^*$, indicative for a lamellar phase. From the position of the principal scattering peak, a principal interplanar (domain) spacing ($d^* = 2\pi/q^*$) of 6.8 nm was calculated.

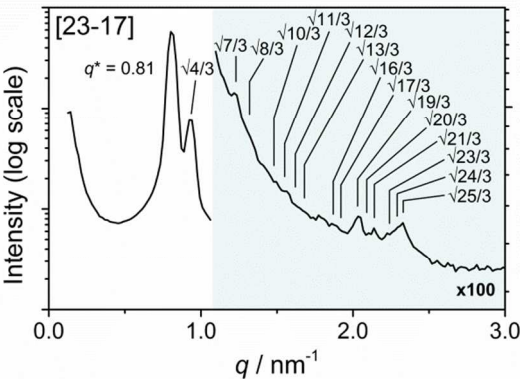


Figure 6: SAXS data for BCO [23-17]. Theoretical higher order Bragg reflections for a gyroid morphology are indicated.

For lamellae, this domain spacing is equal to the inter-lamellar distance (*i.e.*, the sum of the lamellar thicknesses of both co-oligomer constituents), indicating that the lamellar thickness of the individual blocks is approximately 3.4 nm. Similar behaviour was observed for BCO [23-11] (Figure S24). First, a singular, strong scattering peak was visible at $q^* = 0.96 \text{ nm}^{-1}$, without additional Bragg reflections at higher q -values. After aging for 6 months at room temperature,⁶¹ the formation of hexagonally packed cylinders of the minor block (*o*LA) in a matrix of the major block (*o*DMS) was observed, as is evident from additional reflections at $\sqrt{3}q^*$, $\sqrt{4}q^*$ and $\sqrt{7}q^*$. From the value for the domain spacing ($d^* = 6.5 \text{ nm}$), a cylinder-to-cylinder distance ($R_{IC} = 2d^*/\sqrt{3}$) of 7.5 nm was extracted. The diameter of the *o*LA cylinders (D_{CYL}) was estimated to be 4.2 nm with the following relation (see Supporting Material for the derivation of this formula):

$$D_{\text{CYL}} = \left(\frac{8f_{\text{LA}}d^{*2}}{\sqrt{3} \cdot \pi} \right)^{\frac{1}{2}}$$

To the best of our knowledge, the dimensions of the lamellar and cylindrical structures formed by co-oligomers [15-17] and [23-11], respectively, belong to the smallest reported for a pristine diblock BCP system.^{2,4,7,8,60,62-64} This is the more remarkable, since literature typically reports that monodisperse polymers are less able to phase-separate at low χN values.⁶⁵⁻⁶⁷ For BCO [23-13], with two additional lactic acid repeating units, no prolonged aging times were required to generate a micro-phase separated system. The scattering pattern with $q^* = 0.89 \text{ nm}^{-1}$ ($d^* = 7.1 \text{ nm}$) and additional reflections at $\sqrt{4}q^*$ and $\sqrt{7}q^*$ suggest a cylindrical morphology with $R_{\text{IC}} = 8.2 \text{ nm}$ and $D_{\text{CYL}} \approx 4.8 \text{ nm}$. Upon further increasing f_{LA} ([23-15] and [23-17]), characteristic peaks at for instance $\sqrt{4/3}q^*$ and $\sqrt{7/3}q^*$ suggest the adoption of a gyroid morphology. In case of the [23-17] BCO, even the 16th (theoretical) reflection at $\sqrt{25/3}q^*$ could be observed (Figure 6), reflecting the high level of long-range ordering in this sample. A lamellar structure was observed for BCO [23-25], with $d^* = 8.6 \text{ nm}$ ($q^* = 0.73 \text{ nm}^{-1}$) and higher reflections at $\sqrt{4}q^*$ and $\sqrt{9}q^*$. The two 27-siloxane co-oligomers [27-15] and [27-25] showed cylindrical ($d^* = 8.0 \text{ nm}$, $R_{\text{IC}} = 9.2 \text{ nm}$, $D_{\text{CYL}} = 5.4 \text{ nm}$) and lamellar ($d^* = 9.3 \text{ nm}$) morphologies, respectively, in line with the expected structures based on the *o*LA volume fractions (Figures S25-S26). For a selection of polymers, variable temperature SAXS experiments were performed. The observed order-disorder transitions nicely support the transitions observed in the DSC data (see for example Figure S26 for BCO [27-25]). Finally, a cylindrical structure ($d^* = 13.7 \text{ nm}$, $R_{\text{IC}} = 15.8 \text{ nm}$, $D_{\text{CYL}} = 9.0 \text{ nm}$) was found for the longest co-oligomer [59-33] (Figure S27).

Thin-film morphologies. Finally, we evaluated the presence of ordered nanostructures in the co-oligomers [27-15] and [59-33] in a thin film (< 20 nm) by atomic force microscopy (AFM). A uniform, thin polymer film was prepared by spin-coating a 0.6 wt % solution of the BCO in heptane onto a flat silicon substrate with an Anti-Reflective top-Coating (ARC) of 93 nm thick. Important to note here is that no annealing steps were applied after the preparation of the thin layer. The height image of the spin-coated compound [27-15] revealed terrace formation (Figure 7A). Height profiles, extracted from different regions of the image (see for example Figure 7B), indicated that height fluctuations at each terrace were small (< 1 nm). Moreover, a constant height difference was found between two consecutive layers of $8.5 \pm 1 \text{ nm}$. This value is commensurate with the inter-planar spacing that was extracted from the SAXS data for this BCO ($d^* = 8.0 \text{ nm}$). Based on these results and the tendency for this material to form a cylindrical microstructure in bulk, we assume that the film consists of a matrix of *o*DMS, in which *o*LA rich cylinders are present as discrete layers, oriented parallel to the wafer surface (Figure 7C). This is in accordance with previous results obtained with a similar (disperse) PDMS-PLA system⁶ and confirmed by the presence of a fingerprint-like line pattern in the phase image at 500 x 500 nm resolution (Figure 7D). Here, the alternating dark and light lines in this image correspond to the cylinders of *o*LA and the *o*DMS matrix, respectively. A clearer image was obtained at 150 x 150 nm

resolution (inset). Yet, the contrast (*i.e.*, phase difference) remains low (approximately 2 degrees). The low contrast probably is a result of the slight intermixing of the *o*LA and *o*DMS blocks, decreasing the difference in Young's moduli and thus phase difference between the two segregated blocks. Moreover, the surface of the BCO film is anticipated to be covered with a soft and sticky *o*DMS layer, due to the low surface energy of this material with respect to that of *o*LA.^{63,68} This complicates the visualization of the underlying small cylinders.⁶³ Nevertheless, a cylinder-to-cylinder distance of 9.1 nm could be extracted from the phase image by fast Fourier transform (FFT) analysis, which agrees very well with the value found with X-ray scattering ($R_{\text{IC}} = 9.2 \text{ nm}$).

As expected, co-oligomer [59-33] formed a similar type of microstructure, composed of an *o*DMS matrix with *o*LA cylinders ($R_{\text{IC}} = 15.1 \text{ nm}$) parallel to the wafer surface (Figure 7E). Due to the stronger segregation of this longer BCO, a larger phase difference between the *o*LA and *o*DMS blocks was present. Interestingly, less long-range ordering of the *o*LA cylinders was observed when compared to the structure formed by BCO [27-15]. Probably, this decreased order is a direct result of the higher stiffness and thus lower chain mobility of the longer BCO. Indeed, after thermal annealing of the sample for 2 hours in vacuum at 120 °C, a system with better long range ordering was obtained (Figure S28).

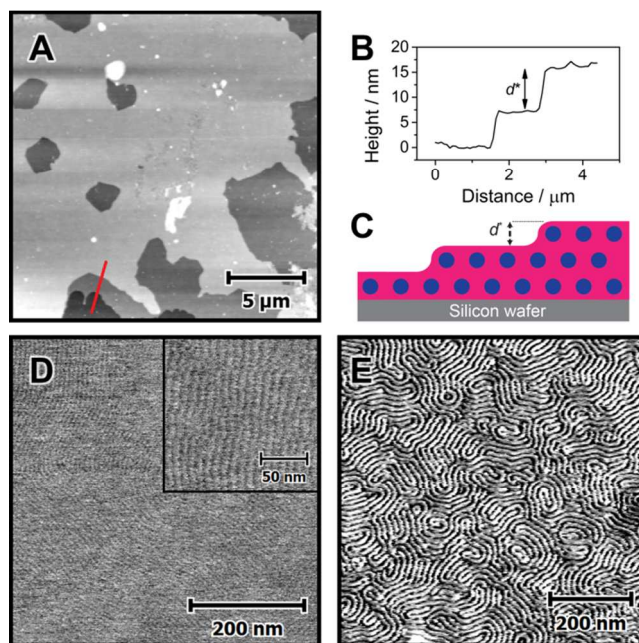


Figure 7: Tapping mode AFM images of BCOs [27-15] (A-D) and [59-33] (E) as thin films on an ARC-modified silicon wafer: A) Height image with B) extracted height profile along the red line and C) cartoon of the cross-section perpendicular to the wafer surface along the red line. Although the cartoon suggests that the *o*DMS block wets the wafer surface, the exact morphology of the wetting layer is unknown. D) Phase image of BCO [27-15] monolayer, including an inset at higher magnification. E) Phase image of BCO [59-33]. (light = *o*LA, dark = *o*DMS).

CONCLUSION

We have demonstrated that an iterative synthesis process with orthogonal protection/deprotection and coupling strategies can be successfully employed to obtain discrete length oligomers of dimethylsiloxane and lactic acid. Subsequent ligation of these blocks afforded *o*DMS-*o*LA diblock co-oligomers of molecular weights up to 6.9 kDa ($DP = 92$) and various *o*LA volume fractions. As a result of the mild and practically neutral conditions that were used during the carbodiimide facilitated ligation and acid chloride formation, practically no degradation of the oligomers took place, resulting in extremely low molar mass dispersities ($D \leq 1.00002$). In principle, this synthesis strategy could be extended to generate even longer BCOs, BCOs composed of a different type of polyester block or BCOs containing moieties that provide additional stabilizing interactions. However, when interested in multigram quantities, the synthesis of the dononacontamer is at present time the limit from the siloxane point of view. Additionally, there is a practical length limit for the individual blocks around 100-150 repeating units due to decreasing reaction rates as a result of end-group dilution. Moreover, ligation of two highly incompatible blocks becomes extremely inefficient at individual oligomer lengths of 50 repeating units and higher. However, much to our surprise, the relatively short BCOs possess already sharp order-disorder transitions of phase-separated morphologies. Although, literature data suggests that lowering the dispersity of block copolymers leads to a higher critical χN_{ODT} value, the present results are obtained with discrete molecules without any dispersity and therefore resemble more organic molecules or liquid crystals. Further research is needed to make this claim more general.

The excellent long-term stability and low order-disorder transition temperatures (T_{ODT}) provides convenient processing conditions for the relatively low MW BCOs at ambient or slightly elevated temperatures. Furthermore, we showed that minor changes in block lengths (i.e. 2 lactic acid units difference) have a major effect on the type of well-ordered microstructures that is formed. With these small changes in composition, we could demonstrate that kinetic effects become increasingly important when approaching the order-disorder barrier for BCOs. Yet, well-defined, extremely small features were obtained in the form of 3.4 nm thin lamellae and cylinders of 4.2 nm in diameter. Also, we managed to obtain clear micrographs of the longest monodisperse BCO [59-33]. In future work, we will further explore the effects of absence of chain length and composition dispersity both on the self-assembly of BCOs in bulk material, thin films and in confined space. Also, we would like to use these materials as perfect model compounds to obtain more accurate values for the thermodynamic parameters that describe the self-assembly behaviour of PDMS-PLA block copolymers. These materials may also serve to strengthen the applicability of ultra-small molar mass BCPs used for lithographic templates, where the adoption of regular patterns is demonstrably impeded by fluctuations and dispersity.^{69,70}

ASSOCIATED CONTENT

Experimental procedures and additional data. This material is available free of charge via the Internet at <http://pubs.acs.org>.

AUTHOR INFORMATION

Corresponding Author

* e.w.meijer@tue.nl

ACKNOWLEDGMENT

This work is financed by the Dutch Ministry of Education, Culture and Science (Gravity program 024.001.035), the Royal Netherlands Academy of Arts and Sciences, and the European Research Council (FP7/2007–2013, ERC Advanced Grant No. 246829). We thank Timo Sciarone for the TGA measurements and we gratefully thank Prof. Craig J. Hawker for discussions and support in the development of the original *o*LA synthesis route.

ABBREVIATIONS

TBDMS, *tert*-butyldimethylsilyl; Bn, benzyl; EDC·HCl, 1-ethyl-3-(3-dimethylaminopropyl)carbodiimide hydrochloride; DPTS, *N,N*-dimethylaminopyridinium *p*-toluene sulfonate; CSA, camphorsulfonic acid; DCTB, trans-2-[3-(4-*tert*-butylphenyl)-2-methyl-2-propenylidene]malono-nitrile.

REFERENCES

- (1) S. H. Kim; M. J. Misner; T. P. Russell. *Adv. Mater.* **2004**, *16*, 2119.
- (2) S. Park; D. H. Lee; J. Xu; B. Kim; S. W. Hong; U. Jeong; T. Xu; T. P. Russell. *Science* **2009**, *323*, 1030.
- (3) M. D. Rodwogin; C. S. Spanjers; C. Leighton; M. a. Hillmyer. *ACS Nano* **2010**, *4*, 725.
- (4) J. D. Cushen; C. M. Bates; E. L. Rausch; L. M. Dean; S. X. Zhou; C. G. Willson; C. J. Ellison. *Macromolecules* **2012**, *45*, 8722.
- (5) J. D. Cushen; I. Otsuka; C. M. Bates; S. Halila; S. Fort; C. Rochas; J. A. Easley; E. L. Rausch; A. Thio; R. Borsali; C. G. Willson; C. J. Ellison. *ACS Nano* **2012**, *6*, 3424.
- (6) L. M. Pitet; S. F. Wuister; E. Peeters; E. J. Kramer; C. J. Hawker; E. W. Meijer. *Macromolecules* **2013**, *46*, 8289.
- (7) D. P. Sweat; M. Kim; S. R. Larson; J. W. Choi; Y. Choo; C. O. Osuji; P. Gopalan. *Macromolecules* **2014**, *47*, 6687.
- (8) J. G. Kennemur; L. Yao; F. S. Bates; M. A. Hillmyer. *Macromolecules* **2014**, *47*, 1411.
- (9) I. Keen; H.-H. Cheng; A. Yu; K. S. Jack; T. R. Younkin; M. J. Leeson; A. K. Whittaker; I. Blakey. *Macromolecules* **2014**, *47*, 276.
- (10) H.-C. Lee; H.-Y. Hsueh; U.-S. Jeng; R.-M. Ho. *Macromolecules* **2014**, *47*, 3041.
- (11) E. A. Jackson; M. A. Hillmyer. *ACS Nano* **2010**, *4*, 3548.
- (12) X. Qiu; H. Yu; M. Karunakaran; N. Pradeep; S. P. Nunes; K.-V. Peinemann. *ACS Nano* **2013**, *7*, 768.
- (13) Y. Kang; J. J. Walsh; T. Gorishnyy; E. L. Thomas. *Nat. Mater.* **2007**, *6*, 957.
- (14) S. B. Darling. *Energy Environ. Sci.* **2009**, *2*, 1266.
- (15) L. Leibler. *Macromolecules* **1980**, *13*, 1602.
- (16) P. Chen; H. Liang; A.-C. Shi. *Macromolecules* **2007**, *40*, 7329.
- (17) M. W. Matsen; F. S. Bates. *Macromolecules* **1996**, *29*, 1091.
- (18) M. W. Matsen; F. S. Bates. *J. Polym. Sci. Part B Polym. Phys.* **1997**, *35*, 945.

- (19) B. Yu; B. Li; Q. Jin; D. Ding; A.-C. Shi. *Soft Matter* **2011**, 7, 10227.
- (20) W. J. Durand; G. Blachut; M. J. Maher; S. Sirard; S. Tein; M. C. Carlson; Y. Asano; S. X. Zhou; A. P. Lane; C. M. Bates; C. J. Ellison; C. G. Willson. *J. Polym. Sci. Part A Polym. Chem.* **2015**, 53, 344.
- (21) N. A. Lynd; M. A. Hillmyer. *Macromolecules* **2005**, 38, 8803.
- (22) M. W. Matsen. *Eur. Phys. J. E* **2013**, 36, 44.
- (23) T. M. Beardsley; M. W. Matsen. *Macromolecules* **2011**, 44, 6209.
- (24) M. Matsen. *Phys. Rev. Lett.* **2007**, 99, 148304.
- (25) J.-F. Lutz; M. Ouchi; D. R. Liu; M. Sawamoto. *Science* **2013**, 341, 1238149.
- (26) S. Park; K. Kwon; D. Cho; B. Lee; M. Ree; T. Chang. *Macromolecules* **2003**, 36, 4662.
- (27) J. Sun; A. A. Teran; X. Liao; N. P. Balsara; R. N. Zuckermann. *J. Am. Chem. Soc.* **2014**, 136, 2070.
- (28) J. Sun; A. A. Teran; X. Liao; N. P. Balsara; R. N. Zuckermann. *J. Am. Chem. Soc.* **2013**, 135, 14119.
- (29) O. I. Paynter; D. J. Simmonds; M. C. Whiting. *J. Chem. Soc. Chem. Commun.* **1982**, 1165.
- (30) I. Bidd; M. C. Whiting. *J. Chem. Soc. Chem. Commun.* **1985**, 543.
- (31) G. M. Brooke; S. Burnett; S. Mohammed; D. Proctor; M. C. Whiting. *J. Chem. Soc. Perkin Trans. 1* **1996**, 1635.
- (32) K. S. Lee; G. Wegner. *Die Makromol. Chemie, Rapid Commun.* **1985**, 6, 203.
- (33) R. Fordyce; E. L. Lovell; H. Hibbert. *J. Am. Chem. Soc.* **1939**, 61, 1905.
- (34) F. A. Loiseau; K. K. Hii; A. M. Hill. *J. Org. Chem.* **2004**, 69, 639.
- (35) S. A. Ahmed; M. Tanaka. *J. Org. Chem.* **2006**, 71, 9884.
- (36) A. C. French; A. L. Thompson; B. G. Davis. *Angew. Chem. Int. Ed. Engl.* **2009**, 48, 1248.
- (37) G. Székely; M. Schaeperstoens; P. R. J. Gaffney; A. G. Livingston. *Chemistry* **2014**, 20, 10038.
- (38) Y. Li; Q. Guo; X. Li; H. Zhang; F. Yu; W. Yu; G. Xia; M. Fu; Z. Yang; Z.-X. Jiang. *Tetrahedron Lett.* **2014**, 55, 2110.
- (39) W. Shi; A. J. McGrath; Y. Li; N. A. Lynd; C. J. Hawker; G. H. Fredrickson; E. J. Kramer. *Macromolecules* **2015**, 48, 3069.
- (40) V. Percec; A. D. Asandei. *Macromolecules* **1997**, 30, 7701.
- (41) C. J. Hawker; E. E. Malmström; C. W. Frank; J. P. Kampf. *J. Am. Chem. Soc.* **1997**, 119, 9903.
- (42) U. D. Lengweiler; M. G. Fritz; D. Seebach. *Helv. Chim. Acta* **1996**, 79, 670.
- (43) J. B. Williams; T. M. Chapman; D. M. Hercules. *Macromolecules* **2003**, 36, 3898.
- (44) K. Takizawa; C. Tang; C. J. Hawker. *J. Am. Chem. Soc.* **2008**, 130, 1718.
- (45) K. Takizawa; H. Nulwala; J. Hu; K. Yoshinaga; C. J. Hawker. *J. Polym. Sci. Part A Polym. Chem.* **2008**, 46, 5977.
- (46) N. Aratani; A. Osuka; Y. H. Kim; D. H. Jeong; D. Kim. *Angew. Chemie Int. Ed.* **2000**, 39, 1458.
- (47) K. Inouchi; S. Kobashi; K. Takimiya; Y. Aso; T. Otsubo. *Org. Lett.* **2002**, 4, 2533.
- (48) T. Izumi; S. Kobashi; K. Takimiya; Y. Aso; T. Otsubo. *J. Am. Chem. Soc.* **2003**, 125, 5286.
- (49) N. Aratani; A. Takagi; Y. Yanagawa; T. Matsumoto; T. Kawai; Z. S. Yoon; D. Kim; A. Osuka. *Chem. – A Eur. J.* **2005**, 11, 3389.
- (50) F. P. V. Koch; P. Smith; M. Heeney. *J. Am. Chem. Soc.* **2013**, 135, 13695.
- (51) F. Zeng; S. C. Zimmerman. *Chem. Rev.* **1997**, 97, 1681.
- (52) L. M. Pitet; A. H. M. van Loon; E. J. Kramer; C. J. Hawker; E. W. Meijer. *ACS Macro Lett.* **2013**, 2, 1006.
- (53) H. Uchida; Y. Kabe; K. Yoshino; A. Kawamata; T. Tsumuraya; S. Masamune. *J. Am. Chem. Soc.* **1990**, 112, 7077.
- (54) P. L. Brown; F. J. Hyde. Linear Chlorosiloxanes. US3235579, 1966.
- (55) K. A. Andrianov; V. V. Astakhin; V. K. Pyzhov. *Bull. Acad. Sci. USSR Div. Chem. Sci.* **1962**, 11, 2144.
- (56) M. Eggen; S. K. Nair; G. I. Georg. *Org. Lett.* **2001**, 3, 1813.
- (57) B. D. Karstedt. Platinum complexes of unsaturated siloxanes and platinum containing organopolysiloxanes. US3775452, 1973.
- (58) A. Devos; J. Remion; A.-M. Frisque-Hesbain; A. Colens; L. Ghosez. *J. Chem. Soc. Chem. Commun.* **1979**, 1180.
- (59) J. K. Kim; H. H. Lee; Q.-J. Gu; T. Chang; Y. H. Jeong. *Macromolecules* **1998**, 31, 4045.
- (60) S. Lee; T. T. M. Gillard; F. S. Bates. *AIChE J.* **2013**, 59, 3502.
- (61) No kinetic measurements were performed; the aging period of 6 months was taken arbitrarily.
- (62) T. Isono; I. Otsuka; D. Suemasa; C. Rochas; T. Satoh; R. Borsali; T. Kakuchi. *Macromolecules* **2013**, 46, 8932.
- (63) Y. Luo; D. Montarnal; S. Kim; W. Shi; K. P. Barteau; C. W. Pester; P. D. Hustad; M. D. Christianson; G. H. Fredrickson; E. J. Kramer; C. J. Hawker. *Macromolecules* **2015**, 48, 3422.
- (64) C. Sinturel; F. S. Bates; M. A. Hillmyer. *ACS Macro Lett.* **2015**, 4, 1044.
- (65) N. A. Lynd; A. J. Meuler; M. A. Hillmyer. *Prog. Polym. Sci.* **2008**, 33, 875.
- (66) M. W. Matsen. *Phys. Rev. Lett.* **2007**, 99, 148304.
- (67) N. A. Lynd; M. A. Hillmyer. *Macromolecules* **2007**, 40, 8050.
- (68) C. Ringard-Lefebvre; A. Baszkin. *Langmuir* **1994**, 10, 2376.
- (69) L. M. Pitet; E. Alexander-Moonen; E. Peeters; T. S. Druzhinina; S. F. Wuister; N. A. Lynd; E. W. Meijer. *ACS Nano* **2015**, 9, 9594.
- (70) V. Mishra; G. H. Fredrickson; E. J. Kramer. *ACS Nano* **2012**, 6, 2629.

Insert Table of Contents artwork here

